Proceedings of the Institution of Mechanical Engineers, Part D: Journal of Automobile Engineering
http://pid.sagepub.com/

Active suspension systems for vehicles based on a sliding-mode controller in combination with inertial delay control

Vaijayanti S Deshpande, Pramod D Shendge and Shrivijay B Phadke

Proceedings of the Institution of Mechanical Engineers, Part D: Journal of Automobile Engineering published online 21 November 2012
DOI: 10.1177/0954407012462953

Original Article

Institution of MECHANICAL ENGINEERS
Journal of AUTOMOBILE ENGINEERING

Proc IMechE Part D:
J Automobile Engineering
0(0) 1–16

DOI: 10.1177/0954407012462953
pid.sagepub.com
SAGE

Active suspension systems for vehicles based on a sliding-mode controller in combination with inertial delay control

Vaijayanti S Deshpande[1], Pramod D Shendge[2] and Shrivijay B Phadke[2]

Abstract

In this paper a new active suspension scheme for vehicles with non-linearities is proposed. The proposed scheme makes the vehicle suspension system follow a modified skyhook model and is based on the sliding-mode control strategy augmented by the so-called inertial delay control which estimates and negates the effects of the unknown road profile and the uncertainties in the suspension system. The accuracy of estimation is analysed and it is shown that the estimation error is ultimately bounded. The means to improve the accuracy of estimation are outlined and the overall stability of the suspension system is proved. The efficacy of the method is illustrated by simulation for an automobile vehicle suspension system for various road profiles.

Keywords

Active suspension, inertial delay control, sliding mode control, skyhook model

Date received: 22 June 2012; accepted: 31 August 2012

Introduction

One of the major challenges faced by the automobile industry is to develop suspension systems to give ride comfort to passengers on rough roads. A conventional suspension system is a passive system consisting of springs and dampers. Since the suspension is affected by the inherent non-linear behaviour of springs and dampers and since the damping coefficient and the spring stiffness of a passive suspension system are fixed, the performance of a passive suspension is limited. In an active suspension system, an actuator is connected between the sprung mass and the unsprung mass in parallel with a spring and a damper. This produces a force to reduce the displacement and acceleration of the body as well as the wheel hop motion caused by uneven road conditions. Compared with a passive suspension system, an active suspension system has the potential to provide a better ride quality and road-holding ability for a variety of road profiles and therefore it has attracted the attention of control engineers for a long time.

Several diverse control strategies such as optimal control,[1] adaptive control,[2–5] model reference adaptive control, sliding-mode control and fuzzy control[6–8] have been reported in the literature. Model reference adaptive control aims to make the output of an unknown vehicle plant suspension system follow a desired reference model. The skyhook model has been used by many researchers[9–12] as an ideal conceptual suspension reference model.

Sliding-mode control (SMC) is a well-known strategy for handling uncertain systems acted upon by external unmeasurable disturbances. It can guarantee invariance if the bound on uncertainties is known and the matching conditions are satisfied.[13,14] The desired dynamic behaviour of the system can be obtained by making a suitable choice of the sliding surface. SMC in combination with model reference control was used by Mohan and co-workers.[10,11] In the paper by Kim and Ro[12] a sliding-mode controller for vehicles with non-linearities was proposed.

In general, it is difficult to find an accurate model of a real suspension system. It is even more difficult to find a good estimate of the road disturbance. Notable contributions to address the issue of estimation of the road

[1]NBN Sinhgad Technical Institutes Campus, Sinhgad Technical Education Society, Pune, India
[2]College of Engineering Pune, Shivajinagar, Pune, India

Corresponding author:
Shrivijay B Phadke, Department of Instrumentation and Control, College of Engineering Pune, Shivajinagar, Pune 411005, India.
Email: sbp.instru@coep.ac.in

disturbance are the function approximation[15,16] and the design of observers.[17] Some other methods such as time delay control[18] (which uses information in the recent past to estimate the uncertainties and disturbances), the uncertainty and disturbance estimator[19–21] and the disturbance observer[22] have the potential to provide estimates of the uncertainties and the road disturbance. All these methods have found several applications in missile autopilots, missile guidance, robotics and several other fields but no application to an active suspension has been reported in the literature.

In this paper, an active suspension system that follows a skyhook model using SMC together with a method called inertial delay control (IDC) (in analogy with time delay control) developed on the lines suggested by Talole and Phadke[20] for a quarter-car suspension system is proposed. A preliminary version was based on the idea appearing in the paper by Deshpande and Phadke.[23] In conventional SMC, the uncertainties and disturbances can be compensated only if their bounds are known. In the present problem, obtaining such bounds is difficult because the road disturbance can vary considerably, even in a short journey.

In this paper, IDC is employed to estimate the non-linear spring force, the damping force and the effect of the unknown road disturbance. The main contributions of this paper are as follows.

1. The proposed scheme estimates the effects of the road disturbance and other uncertainties and then negates them using control. Therefore the proposed scheme can give a response that is as good as the skyhook suspension system irrespective of the road conditions.
2. No knowledge of bounds on the uncertainties and disturbances is required.
3. Unlike other skyhook reference model schemes proposed in the literature, the proposed scheme does not need real-time integration of an explicit skyhook model, reducing the controller complexity considerably.

The rest of the paper is organized as follows: the second section discusses the quarter-car vehicle model and the reference model. The third section describes the sliding surface and the control design. In the fourth section the control strategy of using IDC is discussed, and in the fifth section the stability is proved and the ultimate bounds on the estimation error are calculated. The efficacy of the proposed controller is illustrated by simulation and the results are discussed in the sixth section.

The implementation issues are discussed in the seventh section, and the conclusion is given in the eighth section.

Problem statement

In this section, the non-linear quarter-car model and the skyhook reference model are discussed.

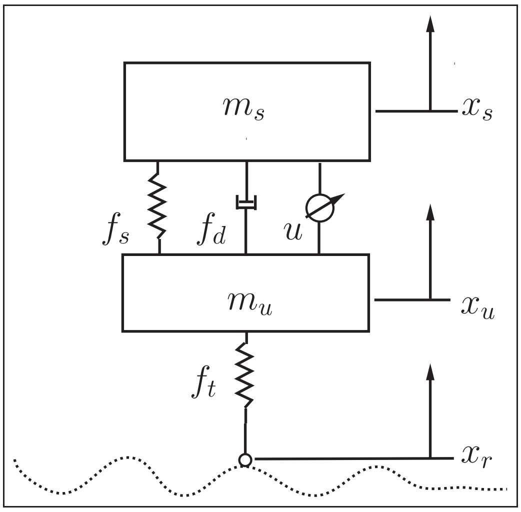

Figure 1. The quarter-car suspension model.

The quarter-car model

Consider a non-linear quarter-car model of a vehicle suspension system as shown in Figure 1. This model is similar to that used by Kim and Ro.[12] The vertical forces on the sprung and unsprung masses are considered. It is assumed that vehicle moves with a constant speed. In a passive suspension system, the sprung mass and the unsprung mass are connected by springs and dampers having constant force coefficients. In an active suspension system, an actuator is connected between the sprung mass and the unsprung mass in parallel with the springs and dampers. The objective of the control strategy is to make the actuator develop a force in such a way as to increase the ride comfort while maintaining good road holding.

The suspension system is described by

$$m_s\ddot{x}_s = -f_s - f_d + u \tag{1}$$

$$m_u\ddot{x}_u = f_s + f_d - f_t - u \tag{2}$$

where m_s is the nominal sprung mass, m_u is the nominal unsprung mass, x_s is the displacement of the sprung mass relative to its static position, x_u is the displacement of the unsprung mass relative to its static position, x_r is the uneven road profile relative to plane ground, f_s is the non-linear spring force, f_d is the non-linear damping force, f_t is the tyre force and u is the control force generated by the actuator. The spring force f_s is given by

$$f_s = k_1\,\Delta x + k_2\,\Delta x^2 + k_3\,\Delta x^3 \tag{3}$$

where the coefficients k_1, k_2 and k_3 are constants and $\Delta x = x_s - x_u$ is the suspension deflection, and the damping force f_d is given by

$$f_d = c_1\,\Delta\dot{x} + c_2\,\Delta\dot{x}^2 \tag{4}$$

where the coefficients c_1 and c_2 are constants. When the tyre loses contact with the ground, the force exerted by the tyre becomes zero. The tyre force f_t is calculated as

$$f_t = \begin{cases} k_t(x_u - x_r) & \text{if } x_u - x_r < \frac{(m_s + m_u)g}{k_t} \\ 0 & \text{if } x_u - x_r \geqslant \frac{(m_s + m_u)g}{k_t} \end{cases} \quad (5)$$

where g is the acceleration due to gravity and k_t is the tyre spring constant. Let the state variables be denoted as $x_1 = x_s$, $x_2 = \dot{x}_s$, $x_3 = x_u$ and $x_4 = \dot{x}_u$. The dynamics represented by equations (1) and (2) can be expressed in the state variable form as

$$\dot{x}_1 = x_2 \quad (6)$$

$$\dot{x}_2 = \frac{1}{m_s}(-f_s - f_d + u) \quad (7)$$

$$\dot{x}_3 = x_4 \quad (8)$$

$$\dot{x}_4 = \frac{1}{m_u}(f_s + f_d - f_t - u) \quad (9)$$

The skyhook reference model

The well-known conceptual skyhook damping system is chosen as the reference model to be followed by the suspension system, as shown in Figure 2. In the skyhook model a damper is connected between the sprung mass and the virtual reference sky. This damper reduces the vibrations of the vehicle but cannot be realized as it is in a real plant. Later, it will be shown how the real plant can be made to behave like the conceptual skyhook model.

As stated by Kim and Ro,[12] the skyhook model is normally excited by the road disturbance but it is difficult to measure the road profile. Since the tyre is almost ten times stiffer than the suspension spring, the displacement of the unsprung mass is a good approximation of the road input within the normal operating frequency range of the suspension system. Therefore the measured states of the unsprung mass can be used as an input to the skyhook reference model. Noting that

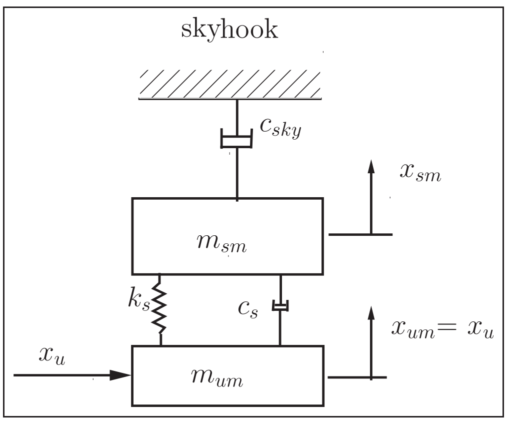

Figure 2. The skyhook reference model.

$x_{um} = x_u = x_3$, the dynamics of sprung mass of the skyhook reference model are given by

$$m_{sm}\ddot{x}_{sm} = -k_s(x_{sm} - x_{um}) - c_s(\dot{x}_{sm} - \dot{x}_{um}) - c_{sky}\dot{x}_{sm} \quad (10)$$

$$= -k_s(x_{sm} - x_3) - c_s(\dot{x}_{sm} - x_4) - c_{sky}\dot{x}_{sm} \quad (11)$$

where c_{sky} is the skyhook linear damper coefficient, m_{sm} is the sprung mass, m_{um} is the unsprung mass, k_s is the linear spring coefficient, c_s is the linear damper coefficient, x_{sm} is the displacement of the sprung mass of the skyhook reference model relative to its static position and x_{um} is the displacement of the unsprung mass of the skyhook reference model relative to its static position.

The sliding surface and the control design

In this section a special sliding surface is selected and a control scheme is designed. The control is designed in such a way that sliding occurs and the sliding surface is chosen in such a way that, when sliding occurs, the system follows the skyhook reference model.

The sliding surface

Select the sliding surface as

$$\sigma = x_2 + z, \qquad z(0) = -x_2(0) \quad (12)$$

The auxiliary variable z is defined as

$$\dot{z} = -\frac{1}{m_{sm}}\left[-k_s(x_1 - x_3) - c_s(x_2 - x_4) - c_{sky}x_2\right] \quad (13)$$

A sliding surface of the type (12) has the advantage that it eliminates the reaching phase and gives full-order sliding.[24] It can be seen that the choice of the dynamics (13) of the auxiliary variable z ensures that the system follows the skyhook reference model. Further the sliding surface used here has the advantage of reducing the complexity of the controller by avoiding integration of an explicit model.

The control design

In this section, the control is designed so that the sliding condition is satisfied. The control u is designed by splitting it into two parts, namely u_{eq} to take care of the known terms and u_n to take care of the uncertainty in equation (15). The control strategy is to use IDC, which is explained in the fourth section, to estimate the uncertainty and then to set u_n equal to the opposite of the estimate of the uncertainty. Differentiating equation (12) and using equations (7) and (13) give

$$\dot{\sigma} = \frac{1}{m_s}(-f_s - f_d + u) - \frac{1}{m_{sm}}\left[-k_s(x_1 - x_3) - c_s(x_2 - x_4) - c_{sky}x_2\right] \quad (14)$$

$$= \frac{1}{m_s}e + \frac{1}{m_s}u - \frac{1}{m_{sm}}\left[-k_s(x_1 - x_3) - c_s(x_2 - x_4) - c_{sky}x_2\right] \tag{15}$$

where $e = -f_s - f_d$ is the lumped uncertainty. The function e depends on the uncertainties and the effect of the road disturbance.

The control u split into parts is given by

$$u = u_{eq} + u_n \tag{16}$$

with

$$u_{eq} = \frac{m_s}{m_{sm}}\left[-k_s(x_1 - x_3) - c_s(x_2 - x_4) - c_{sky}x_2\right] - m_s K\sigma \tag{17}$$

where K is a positive number. Using equations (16) and (17) in equation (15) gives

$$\dot{\sigma} = \frac{1}{m_s}e - K\sigma + \frac{1}{m_s}u_n \tag{18}$$

Let

$$u_n = -\hat{e} \tag{19}$$

where $\hat{e}$ is the estimate of the uncertainty e. In this section, it is assumed that the estimate $\hat{e}$ is available. The fourth section explains how the estimate $\hat{e}$ is obtained. Substituting equation (19) in equation (18), we obtain

$$\dot{\sigma} = -K\sigma + \frac{1}{m_s}e - \frac{1}{m_s}\hat{e} \tag{20}$$

Defining the estimation error as

$$\tilde{e} = e - \hat{e} \tag{21}$$

leads to

$$\dot{\sigma} = -K\sigma + \frac{1}{m_s}\tilde{e} \tag{22}$$

In the next section, an estimator is designed to estimate the lumped uncertainty e.

Inertial delay control

In this section, the idea behind IDC-based control is briefly introduced. The key idea in control is to use the system information in the recent past to obtain an estimate of the uncertainty and then to use the opposite of it in control to negate the effect of the uncertainty.[19,20] For the estimation error $\tilde{e}$ to be bounded, the following assumption is needed.

Assumption 1. The lumped uncertainty e is such that $|\mathrm{d}^{(r)}e/\mathrm{d}t^{(r)}| = |e^{(r)}| \leqslant \mu$, where r is a positive integer and μ is a small positive number.

The lumped uncertainty e can be estimated as

$$\hat{e} = G_f(s)e \tag{23}$$

where $G_f(s)$ is a filter with sufficiently large bandwidth. The order of the filter $G_f(s)$ is defined as the order of the denominator polynomial of $G_f(s)$. Consider a first-order filter which is of the form

$$G_f(s) = \frac{1}{1 + \tau s} \tag{24}$$

where τ is a small positive constant. From equation (20),

$$e = m_s(\dot{\sigma} + K\sigma) + \hat{e} \tag{25}$$

Using equation (25) in equation (23), we obtain

$$\hat{e} = m_s(\dot{\sigma} + K\sigma)G_f(s) + \hat{e}G_f(s) \tag{26}$$

which can be written in the time domain for the first-order filter given by equation (24) as

$$\tau\dot{\hat{e}} + \hat{e} = m_s(\dot{\sigma} + K\sigma) + \hat{e} \tag{27}$$

This simplifies to

$$\hat{e} = \frac{m_s}{\tau}\sigma + \frac{m_s K}{\tau}\int_0^t \sigma \, \mathrm{d}t \tag{28}$$

From equations (21), (23) and (24), we can obtain

$$\dot{\tilde{e}} = -\tfrac{1}{\tau}\tilde{e} + \dot{e} \tag{29}$$

If $\dot{e} = 0$, $\tilde{e}$ goes to zero asymptotically; otherwise it is ultimately bounded. The ultimate boundedness of $\tilde{e}$ and the calculation of the bound on $\tilde{e}$ are discussed in the fifth section. If $\dot{e}$ is not small but $\ddot{e}$ is small, i.e. $r = 2$ in Assumption 1, then the accuracy of estimation can be improved by estimating e as well as $\dot{e}$. The details are shown below.

Improvement in the accuracy of estimation

Let $\hat{e}_1$ be the estimate of e, and $\hat{e}_2 = \dot{\hat{e}}_1$ be the estimate of $\dot{e}$. The corresponding estimation error vector $\tilde{e}$ is defined as

$$\tilde{e} = [\,\tilde{e}_1 \;\; \tilde{e}_2\,]^{\mathrm{T}} \tag{30}$$

where

$$\tilde{e}_1 = e - \hat{e}_1 \tag{31}$$

$$\begin{aligned}\tilde{e}_2 &= \dot{e} - \dot{\hat{e}}_1 \\ &= \dot{e} - \hat{e}_2\end{aligned} \tag{32}$$

The required estimation can be accomplished using a second-order filter of the form

$$G_f(s) = \frac{1 + 2\tau s}{\tau^2 s^2 + 2\tau s + 1} \tag{33}$$

where τ is a small positive constant. Now

$$\hat{e}_1 = G_f(s)e \tag{34}$$

Writing the equations in the time domain with the filter as in equation (33), we find that

$$\tau^2\ddot{\hat{e}}_1 + 2\tau\dot{\hat{e}}_1 + \hat{e}_1 = 2\tau\dot{e} + e$$
$$\tau^2\ddot{\hat{e}}_1 = 2\tau(\dot{e} - \dot{\hat{e}}_1) + e - \hat{e}_1$$
$$\dot{\hat{e}}_2 = \tfrac{2}{\tau}(\dot{e} - \hat{e}_2) + \tfrac{1}{\tau^2}(e - \hat{e}_1) \tag{35}$$

Using the definitions of the estimation errors in equations (31) and (32), we can obtain

$$\dot{\hat{e}}_2 = \frac{2}{\tau}\tilde{e}_2 + \frac{1}{\tau^2}\tilde{e}_1 \tag{36}$$

Subtracting both sides of equation (36) from $\ddot{e}$ and using equation (32) give

$$\dot{\tilde{e}}_2 = -\tfrac{2}{\tau}\tilde{e}_2 - \tfrac{1}{\tau^2}\tilde{e}_1 + \ddot{e} \tag{37}$$

The estimation error equations can be expressed in the state variable form as

$$\begin{aligned}\dot{\tilde{e}}_1 &= \tilde{e}_2\\ \dot{\tilde{e}}_2 &= -\tfrac{2}{\tau}\tilde{e}_2 - \tfrac{1}{\tau^2}\tilde{e}_1 + \ddot{e}\end{aligned} \tag{38}$$

which can be written in the matrix form

$$\dot{\tilde{e}} = M\tilde{e} + N\ddot{e} \tag{39}$$

where

$$\tilde{e} = \begin{bmatrix}\tilde{e}_1\\ \tilde{e}_2\end{bmatrix}, \quad M = \begin{bmatrix}0 & 1\\ -\frac{1}{\tau^2} & -\frac{2}{\tau}\end{bmatrix}, \quad N = \begin{bmatrix}0\\ 1\end{bmatrix} \tag{40}$$

If $\ddot{e} = 0$, $\dot{\tilde{e}}$ goes to zero asymptotically; otherwise it is ultimately bounded as shown in the fifth section. Now the dynamics of the sliding variable (22) are written as

$$\dot{\sigma} = -K\sigma + \tfrac{1}{m_s}\tilde{e}_1 \tag{41}$$

From equations (36), (38) and (41), after some calculation we find that

$$\hat{e}_1 = \frac{2m_s\sigma}{\tau} + \frac{2m_sK}{\tau}\int_0^t \sigma\,\mathrm{d}t + \frac{m_s}{\tau^2}\int_0^t \sigma\,\mathrm{d}t + \frac{m_sk}{\tau^2}\int_0^t\int_0^t \sigma\,\mathrm{d}t\,\mathrm{d}t \tag{42}$$

Stability

In this section, it is proved that the estimation error $\tilde{e}$ and the sliding variable σ are ultimately bounded. Here the more general case when $r = 2$ in Assumption 1 is considered. The bounds on σ and $\tilde{e}$ are found by considering the Lyapunov function as

$$V(\tilde{e}, \sigma) = \tilde{e}^{\mathrm{T}}P\tilde{e} + \tfrac{1}{2}\sigma^2 \tag{43}$$

Taking the derivative of $V(\tilde{e}, \sigma)$ with equations (41) and (39) gives

$$\dot{V}(\tilde{e}, \sigma) = \tilde{e}^{\mathrm{T}}P\dot{\tilde{e}} + \dot{\tilde{e}}^{\mathrm{T}}P\tilde{e} + \sigma\dot{\sigma} \tag{44}$$

$$= \tilde{e}^{\mathrm{T}}(PM + M^{\mathrm{T}}P)\tilde{e} + 2\tilde{e}^{\mathrm{T}}PN\ddot{e} - K\sigma^2 + \sigma\frac{1}{m_s}\tilde{e}_1 \tag{45}$$

Since all eigenvalues of M have negative real parts, we can always find a positive definite matrix P such that

$$PM + M^{\mathrm{T}}P = -Q \tag{46}$$

for a given positive definite matrix Q. Let λ be the smallest eigenvalue of Q. Now $\dot{V}(\tilde{e}, \sigma)$ can be written as

$$\dot{V}(\tilde{e}, \sigma) = -\tilde{e}^{\mathrm{T}}Q\tilde{e} + 2\tilde{e}^{\mathrm{T}}PN\ddot{e} - K\sigma^2 + \sigma\frac{1}{m_s}\tilde{e}_1 \tag{47}$$

$$\leqslant -\lambda\|\tilde{e}\|^2 + 2\|\tilde{e}^{\mathrm{T}}\|\|P\|\|N\||\ddot{e}| - K|\sigma|^2 + \frac{1}{m_s}|\sigma|\|\tilde{e}\| \tag{48}$$

$$\leqslant -\lambda\|\tilde{e}\|^2 - K|\sigma|^2 + \frac{1}{m_s}|\sigma|\|\tilde{e}\| + 2\|\tilde{e}\|\|P\|\|N\|\mu \tag{49}$$

Then, using Young's inequality[25]

$$ab \leqslant \frac{a^2}{2} + \frac{b^2}{2} \tag{50}$$

for any real a and b, we can obtain

$$\dot{V}(\tilde{e}, \sigma) \leqslant -\lambda\|\tilde{e}\|^2 - K|\sigma|^2 + \frac{1}{2m_s}(|\sigma|^2 + \|\tilde{e}\|^2) + 2\|\tilde{e}\|\|P\|\|N\|\mu \tag{51}$$

$$\leqslant -\|\tilde{e}\|^2\left(\lambda - \frac{1}{2m_s}\right) + 2\|\tilde{e}\|\|P\|\|N\|\mu - |\sigma|^2\left(K - \frac{1}{2m_s}\right) \tag{52}$$

$$\leqslant -\|\tilde{e}\|\left[\|\tilde{e}\|\left(\lambda - \frac{1}{2m_s}\right) - 2\|P\|\|N\|\mu\right] - |\sigma|^2\left(K - \frac{1}{2m_s}\right) \tag{53}$$

With $K - 1/2m_s > 0$ and $\lambda - 1/2m_s > 0$, the system will be ultimately bounded. From equation (53) the bound on $\tilde{e}$ becomes

$$\|\tilde{e}\| \leqslant \lambda_1 \leqslant \frac{2\|P\|\|N\|\mu}{\lambda - 1/2m_s} \tag{54}$$

Omitting the calculations the bound on σ gives

$$|\sigma| \leqslant \frac{\lambda_1/m_s + \sqrt{\lambda_1^2/m_s^2 + 8K\lambda_1\|P\|\|N\|\mu}}{2K} \tag{55}$$

Thus the $\|\tilde{e}\|$ and $|\sigma|$ are ultimately bounded and the bounds can be lowered using the control parameters K and τ.

An illustrative example and discussion of the results

The efficacy of the method is verified through computer simulations of the model shown in Figure 1 for a variety of road profiles. The simulation was carried out in the MATLAB and Simulink environment. The plant equations were integrated using the standard fourth-order Runge–Kutta (RK-4) method. For the purposes of control, the auxiliary equation (13) is required to be

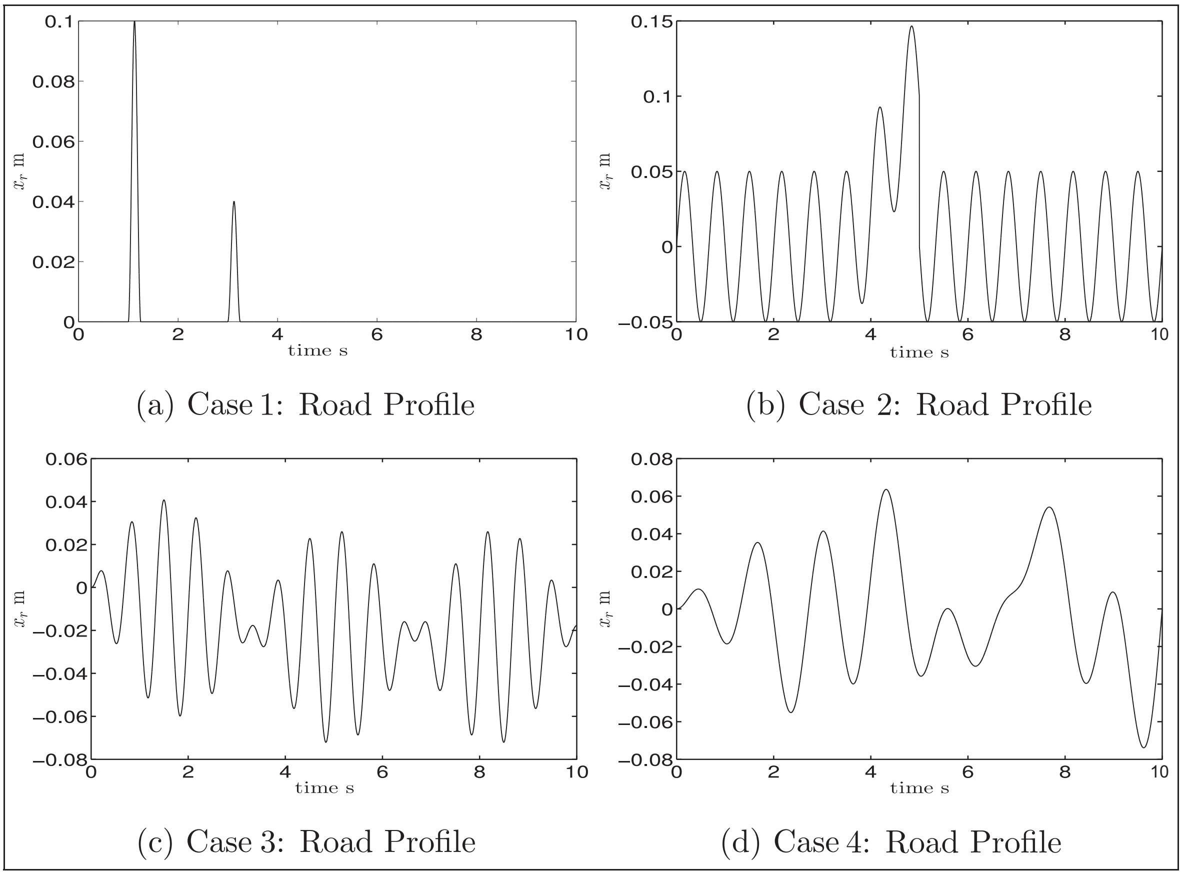

(a) Case 1: Road Profile (b) Case 2: Road Profile

(c) Case 3: Road Profile (d) Case 4: Road Profile

Figure 3. The road profiles considered.
The active and passive suspension systems are simulated for all the four road profiles.

integrated. This was also integrated using the RK-4 method.

The system and control parameters are as follows.

The parameters of the suspension system are $m_s = 240$ kg, $k_t = 150{,}000$ N/m, $k_1 = 12{,}394$ N/m, $k_2 = -73{,}696$ N/m^2, $k_3 = 3{,}170{,}400$ N/m^3, $c_1 = 1385.4$ N s/m, $c_2 = 524.28$ N s^2/m^2 and $m_u = 50$ kg.
The parameters of the skyhook model are $m_{sm} = 240$ kg, $k_s = 15{,}000$ N/m, $c_s = 1860$ N s/m and $c_{sky} = 30{,}000$ N s/m.
The control parameters are $K = 200$ and $\tau = 0.01$ s.
The initial conditions of the plant and model are $x_0 = [0\ 0\ 0\ 0]^T$ and $x_{m0} = [0\ \ 0]^T$ respectively.
Four road profiles were considered for this study, as shown in Figure 3. The specifics of the road profile are given in the appropriate section.

Case 1 road profile

First, the results for the road profile shown in Figure 3(a), referred to as the case 1 road profile, are shown.

This road profile is given by

$$x_r = \begin{cases} 0 & \text{for } 0 \leqslant t < 1 \\ 0.05[1 - \cos(8\pi t)] & \text{for } 1 \leqslant t < 1.25 \\ 0 & \text{for } 1.25 \leqslant t < 3 \\ 0.02[1 - \cos(8\pi t)] & \text{for } 3 \leqslant t < 3.25 \\ 0 & \text{for } 3.25 \leqslant t \end{cases} \tag{56}$$

The active suspension system with first-order IDC is compared with the passive suspension system and the active suspension system with only SMC.

The deflection and the acceleration of the sprung mass are shown in Figure 4 while the suspension deflection and the tyre deflection are shown in Figure 5. The performance with the active suspension is significantly better than that with the passive suspension. The same conclusions were found for the other three profiles as well.

The performance of the active suspension with IDC and that with SMC are very close. However, this is not surprising. In fact, the performance of the controlled system is governed by the chosen skyhook model. A skyhook reference model that gives the desired level of ride comfort while maintaining road holding is chosen. The success in following the model is indicated by the closeness of σ to zero. Any strategy that is successful in making the suspension system follow the skyhook reference system will give the same performance in terms of ride comfort. What is shown here is that σ is ultimately bounded and the ultimate bound is dependent on the control parameters that the user can choose.

The problems with pure SMC are that it needs knowledge of the bounds of the uncertainties and disturbances and that the control is discontinuous, which may cause excessive wear and tear of components. When the discontinuous control is replaced by its

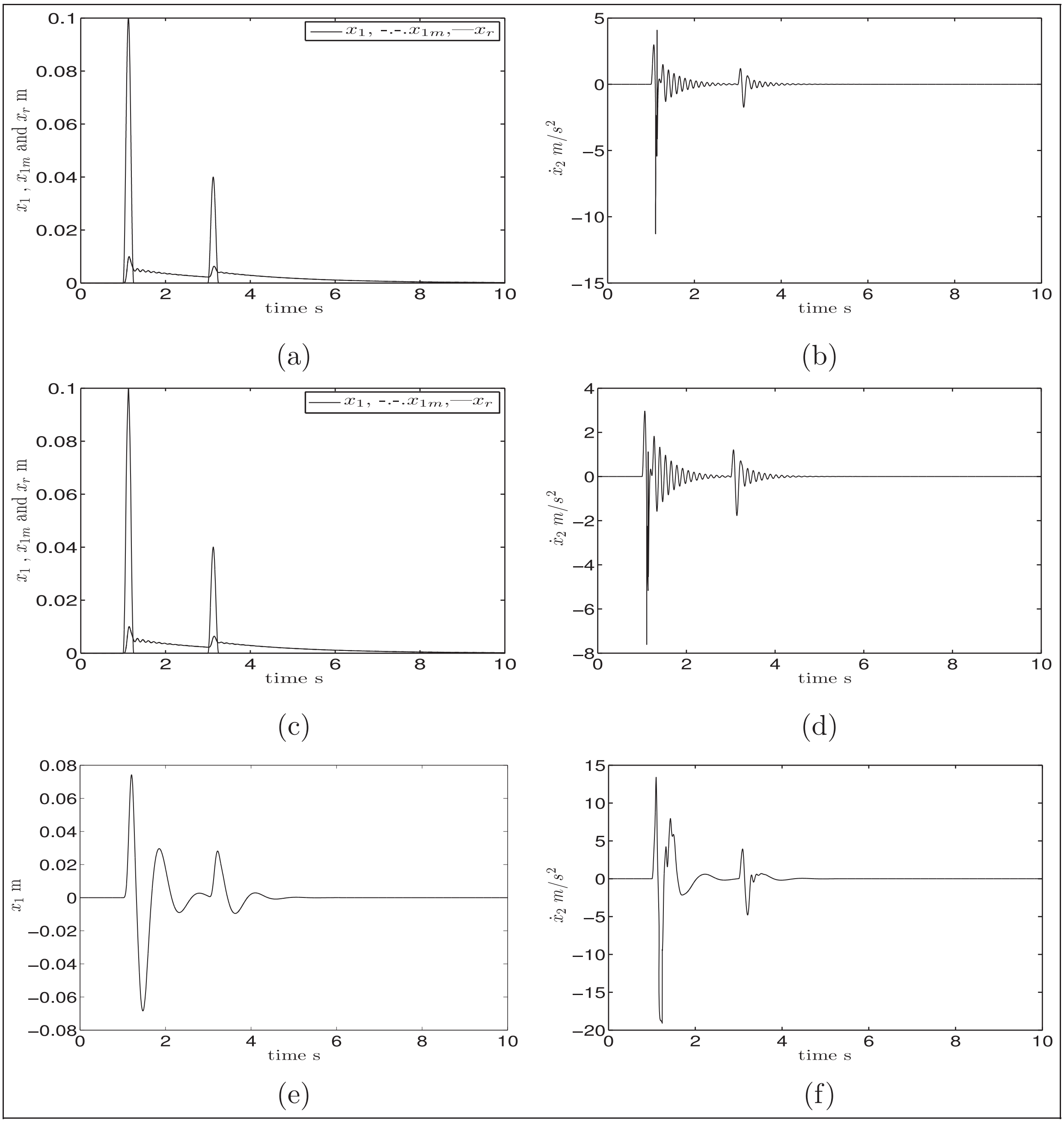

Figure 4. The responses for the case 1 road profile with IDC, SMC and passive suspension: deflection and acceleration of the sprung mass.

smooth approximation, the invariance is compromised. On the other hand, SMC with IDC is an inherently smooth control since the control does not have a discontinuous component. It does not need any knowledge of the uncertainties or their bounds. It may be noted that, in the pure SMC-based design, the nominal parameters were assumed to be known and the uncertainty was assumed to be only 20%. In the case of the pure SMC-based design, the control magnitude increases as the degree of uncertainty increases. The control force u for pure SMC designed on the standard lines is given by

$$u = u_{eq} + u_n \tag{57}$$

with

$$u_{eq} = f_{s0} + f_{d0} + \frac{m_s}{m_{sm}}\left[-k_s(x_1 - x_3) - c_s(x_2 - x_4) - c_{sky}x_2\right] - m_s K\sigma \tag{58}$$

$$u_n = -\rho\,\mathrm{sat}\sigma \tag{59}$$

where K is a positive number, f_{s0} and f_{d0} are the nominal values of the non-linear spring force f_s and the damping force f_d respectively, ρ is the bound of the uncertainties in f_s and f_d, and $\mathrm{sat}\sigma$ is a continuous approximation of the discontinuous signum function. A comparison of the control inputs for SMC with IDC and for only SMC is shown in Figure 6. It can be seen

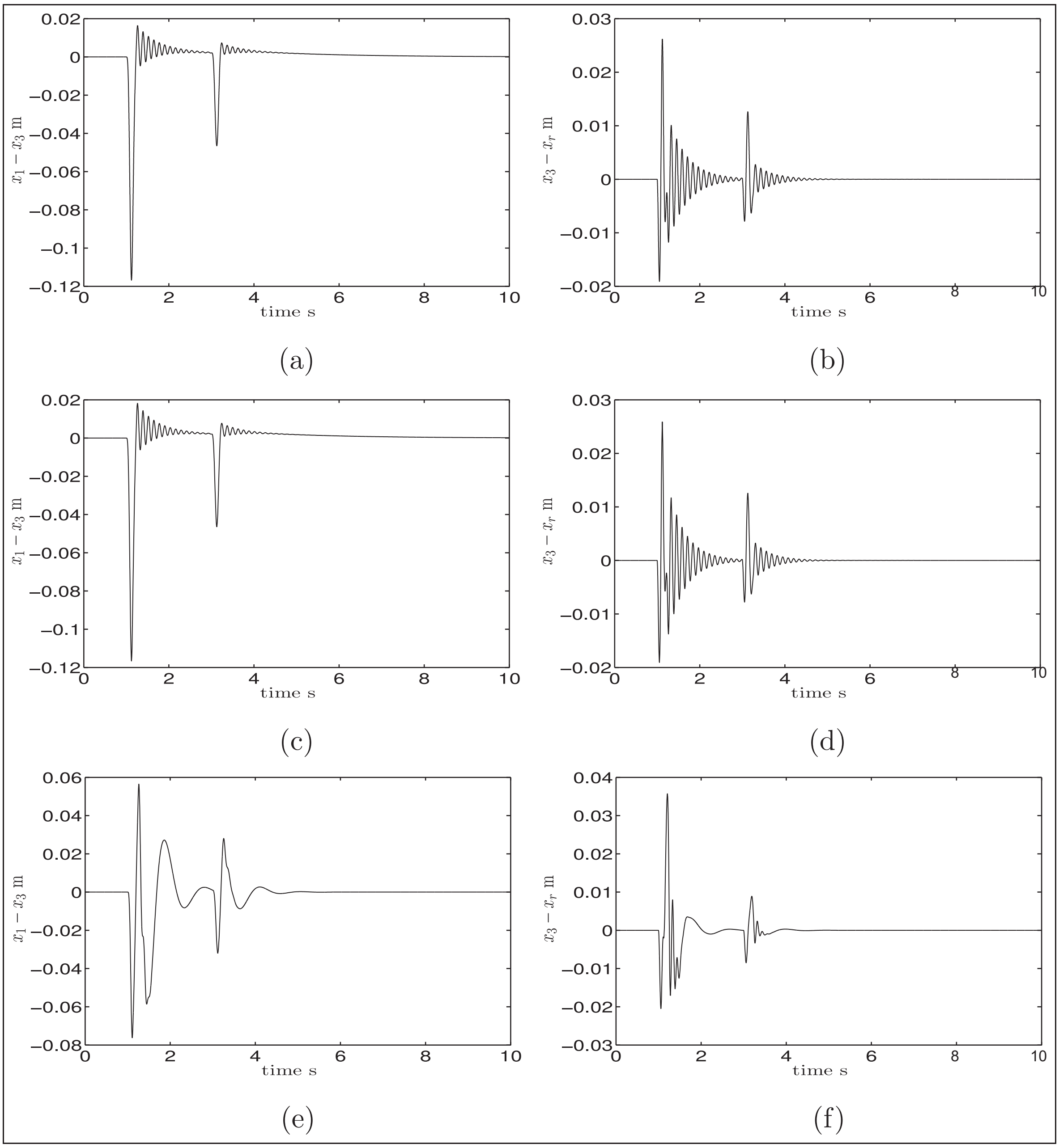

Figure 5. The responses for the case 1 road profile with IDC, SMC and passive suspension: suspension and tyre deflection.

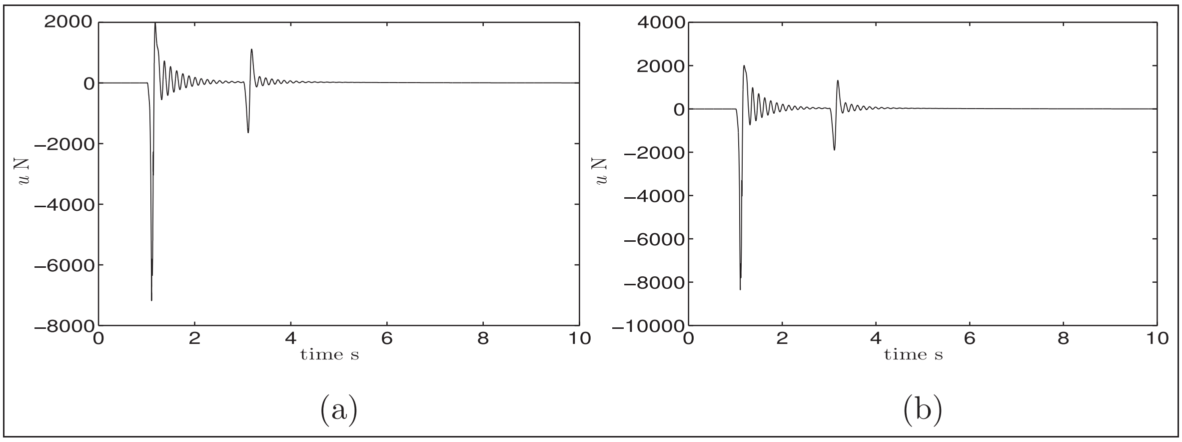

Figure 6. The control inputs for the case 1 road profile for SMC with IDC and for only SMC.

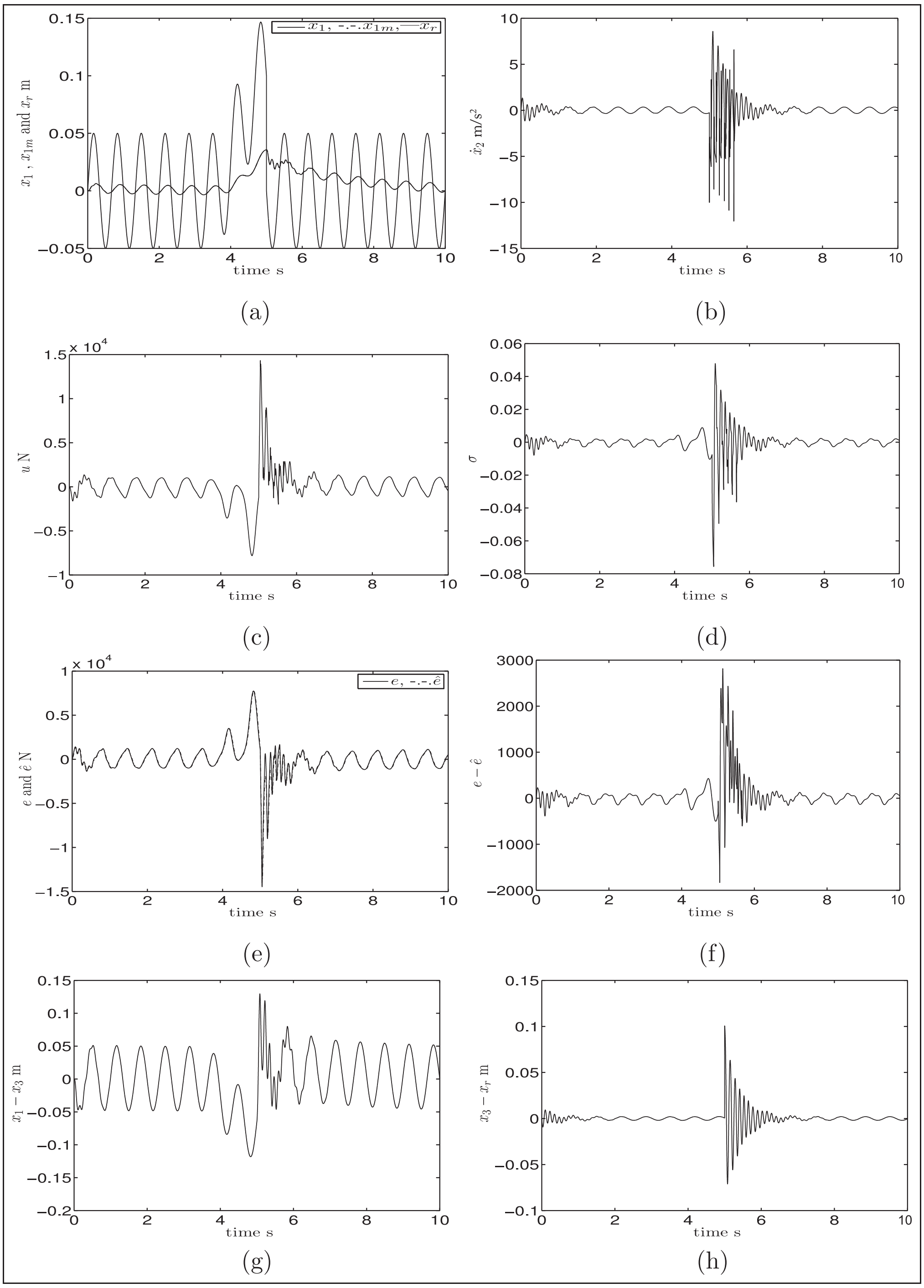

Figure 7. The responses for the case 2 road profile with first-order IDC.

that the control input is slightly larger for control with only SMC for the reasons stated above.

Another comparison between IDC and SMC is shown in the section on the case 4 road profile.

Case 2 road profile

In this section, the suspension system is subjected to the case 2 road profile shown in Figure 3(b). The road profile is generated by

$$x_r = \begin{cases} \mathrm{d}t & \text{for } 0 \leqslant t < 3.5 \\ 0.0592(t-3.5)^3 + 0.1332(t-3.5)^2 + \mathrm{d}t & \text{for } 3.5 \leqslant t < 5 \\ \mathrm{d}t & \text{for } 5 \leqslant t \end{cases} \tag{60}$$

where

$$\mathrm{d}t = 0.05\sin(3\pi t) \tag{61}$$

It should be noted that, after 4 s, this road profile shows a large bump followed by a trough and another large bump immediately.

Figure 7(a) shows that the system follows the skyhook model accurately. For this road profile, the response seen in Figure 7(b) of the acceleration of the sprung mass appears to be high for some period after 4 s. However, it should be noted that the performance is markedly better than it would have been with the passive suspension. This is illustrated by giving the

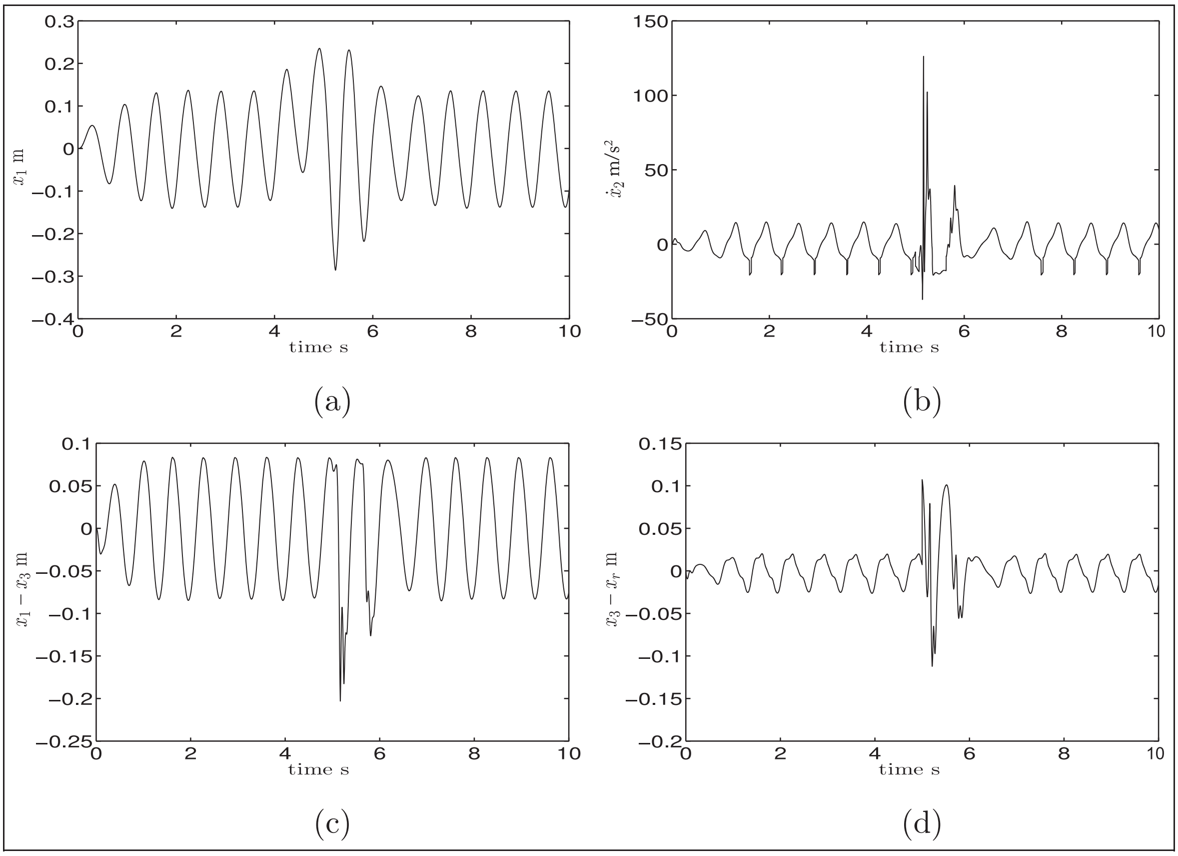

Figure 8. The responses of the passive suspension for the case 2 road profile.

results of the passive suspension for this road profile in Figure 8. The results of the active suspension system are seen to be significantly better in terms of the ride comfort, suspension deflection, sprung-mass deflection and tyre deflection.

Case 3 road profile

In this section, the response of the suspension system is simulated for the case 3 road profile shown in Figure 3(c) which is generated by the equation

$$x_r = 0.05\sin(3\pi t)\sin(0.3\pi t) + 0.025\cos\left(0.075\pi t + \frac{\pi}{2}\right) \tag{62}$$

Like other road profiles, this profile also shows that it follows the skyhook model well, as shown in Figure 9(a). The effectiveness of the IDC scheme in estimating the uncertainty can be seen from Figure 9(f) while the effectiveness with which it follows the model is illustrated by Figure 9(d). The performance of the suspension system is illustrated by the plots of the suspension deflection, sprung-mass acceleration, suspension deflection and tyre deflection shown in Figure 9(a), Figure 9(b), Figure 9(g) and Figure 9(h) respectively.

Case 4 road profile

The performance of IDC for the case 4 road profile shown in Figure 3(d) is illustrated here. This road profile is generated using

$$x_r = 0.05\sin(1.5\pi t)\sin(0.15\pi t) + 0.05\sin(0.6\pi t)\sin(0.03\pi t) \tag{63}$$

From Figure 10(a) it can be seen that the system follows the skyhook reference as desired. Like the case 2 and case 3 road profiles, the control effort and the sliding variable are plotted in Figure 10(c) and Figure 10(d) while the plots of the uncertainty e and its estimate $\hat{e}$ are given in Figure 10(e) and the estimation error is shown in Figure 10(f).

For the case 4 road profile, the responses obtained with IDC-based control are compared with those of pure SMC-based control in Figure 11. It can be seen in Figure 11(a) that the accelerations of the sprung mass are the same for both cases but the sliding variable shown in Figure 11(c) and the control effort shown in Figure 11(b) are better for IDC-based control.

Second-order IDC

The effect of second-order IDC on the accuracy of estimation is considered next. For the case 4 road profile, with the value of τ unchanged, the plots of the uncertainty e and its estimate $\hat{e}$ are shown in Figure 12(a) while the estimation error $\tilde{e}$ is shown in Figure 12(b). It can be seen from Figure 10(f) and Figure 12(b) that second-order IDC improves the accuracy of estimation. The estimation error has decreased by a factor of almost 10.

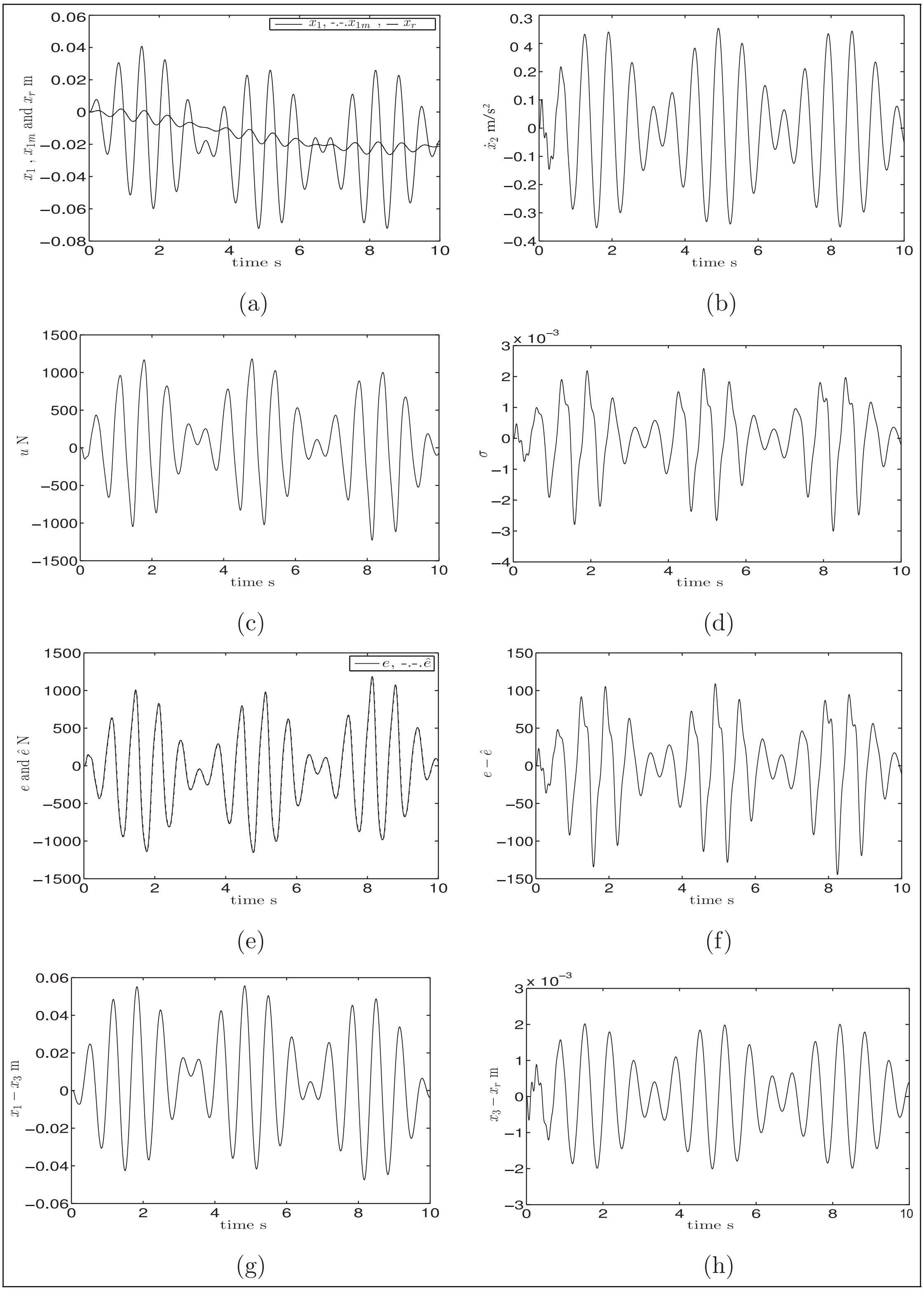

Figure 9. The responses for the case 3 road profile with first-order IDC.

Summary of results

For all the four road profiles, the proposed scheme is successful in giving the performance that the chosen conceptual skyhook reference model would give. Although the four road profiles are significantly different from each other, no change in the control strategy was required. The ride comfort, which was measured by the sprung-mass acceleration and the sprung-mass deflection, and the handling, which was judged from the suspension deflection and the tyre

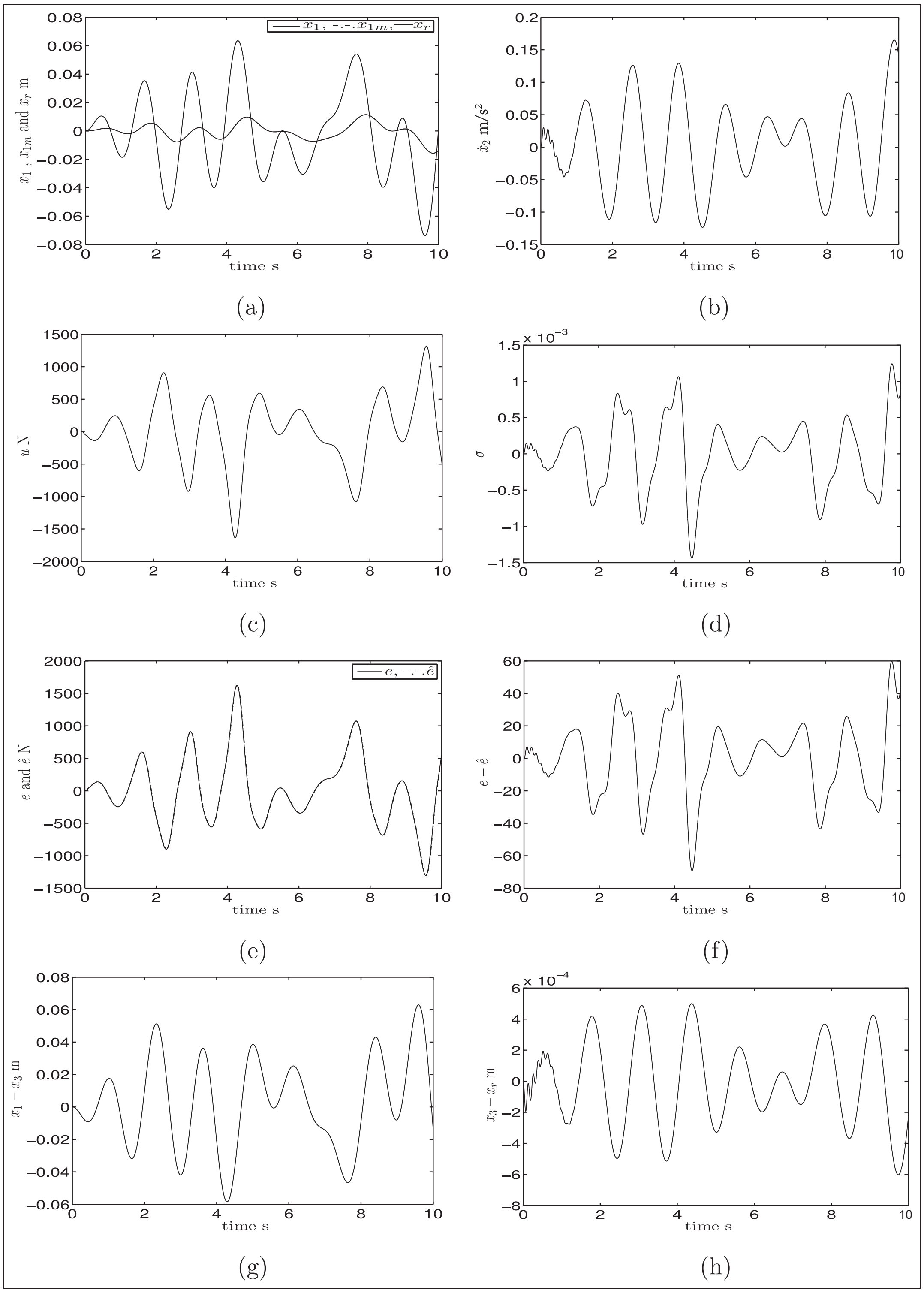

Figure 10. The responses for the case 4 road profile with first-order IDC.

deflection, are far better for the proposed SMC with IDC than for the passive suspension system for all the four road profiles. The scheme based on pure SMC required knowledge of the bounds and the nominal values of the parameters. Second-order IDC improves the accuracy of estimation of the uncertainty by an order of magnitude.

Implementation issues

In this paper, a new active suspension system based on IDC is proposed. In the design and simulation, like many researchers[12,15] proposing a new suspension control strategy, a perfect actuator is assumed to be available for implementing the control. However, in

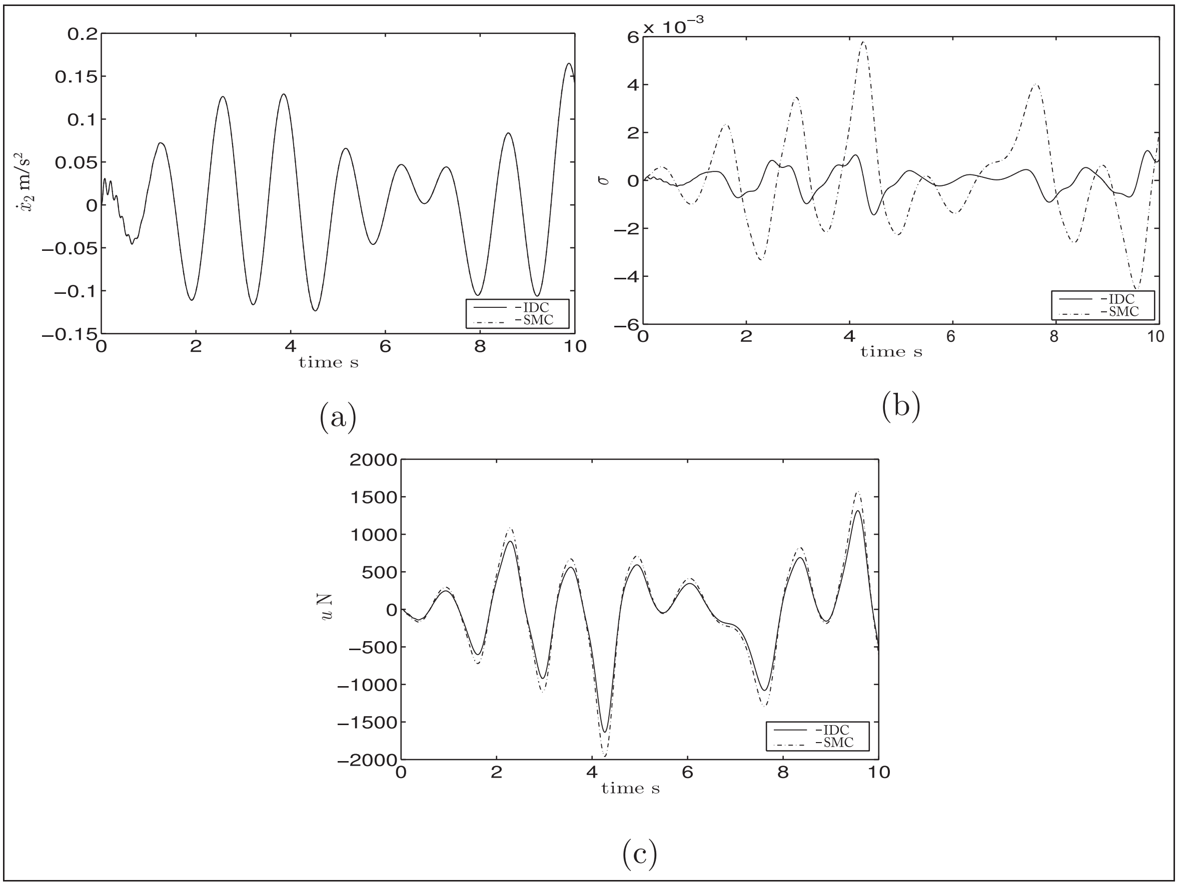

Figure 11. A comparison of the responses of the suspension system with SMC and IDC for the case 4 road profile.

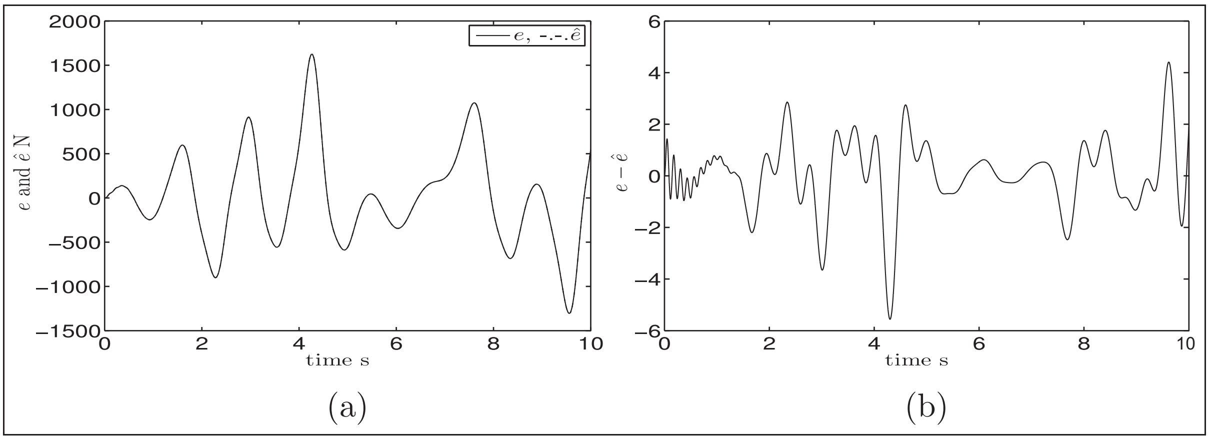

Figure 12. The responses for the case 4 road profile with second-order IDC.

practice, only actuators having small lags can be obtained. For practical implementation, some schemes for actuator compensation have been suggested in the literature.[26,27] Preliminary work carried out by the present authors suggested that the method of IDC proposed here can be extended to incorporate compensation of practical actuators while retaining the performance of the active suspension proposed here.

In the preliminary work, it was seen that, with actuator compensation, the proposed controller can accommodate actuator lags up to 100 ms while retaining the performance of the suspension system. The results with actuator lags of 10 ms, 50 ms and 100 ms with actuator compensation are shown in Figure 13 for the purpose of illustration.

Since the method can be retrofitted to other active suspension strategies developed on the assumption of perfect actuator, it is intended to report this separately.

Another issue that needs to be addressed is the availability of the absolute velocity x_2 of the sprung mass.

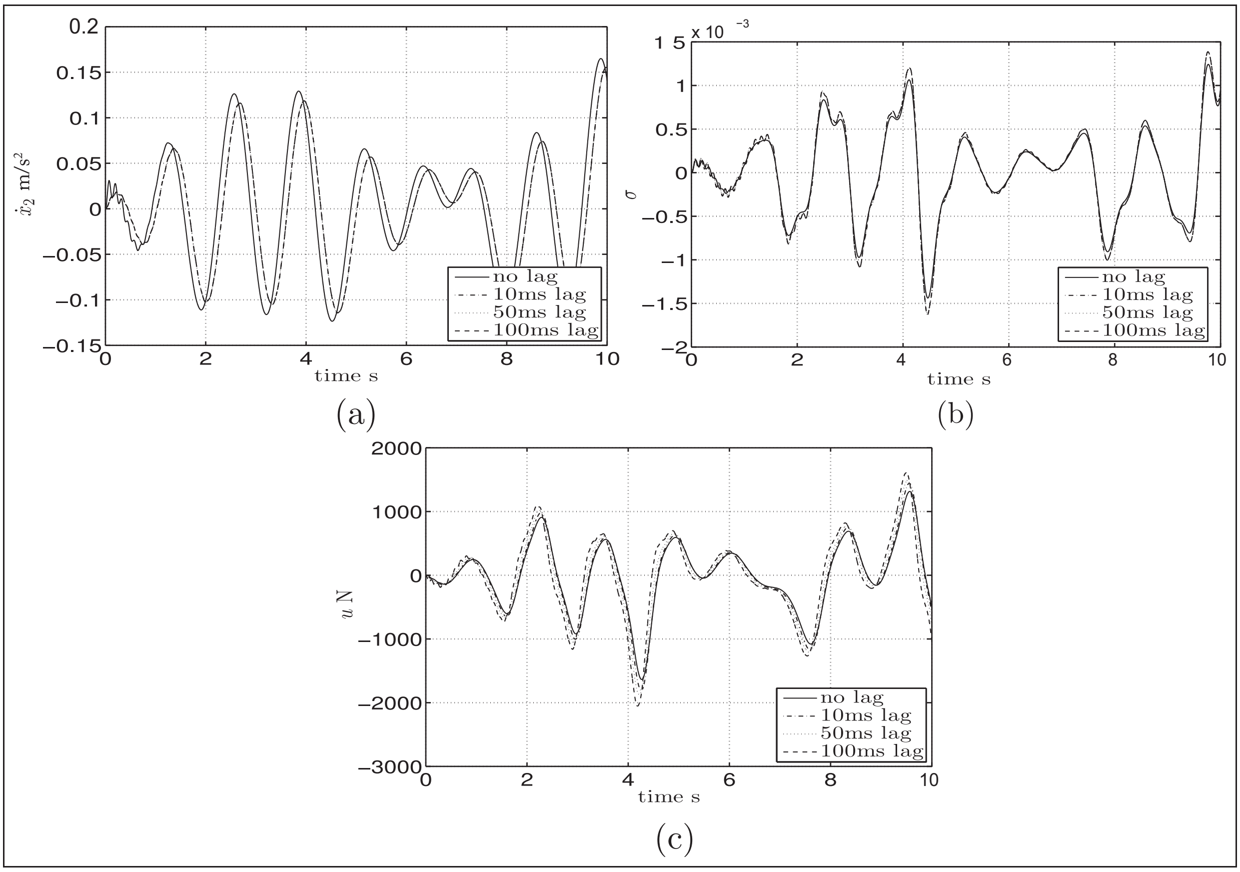

Figure 13. A comparison of the responses of the suspension system with the ideal actuator and in the presence of actuator lags of 10 ms, 50 ms and 100 ms.

This signal is required in the calculation of u_{eq} and the sliding variable σ. As stated by Williams,[28] low-cost transducers capable of measurement of the skyhook velocity are difficult to obtain. The most common solution is to integrate the vertical acceleration to obtain the sprung-mass velocity. This scheme and similar schemes have also been suggested by Truscott,[4] Lin et al.[29] and Preumont et al.,[30] and several other results have been reported in the literature. There are also other methods such as the microelectromechanical system (MEMS) velocity sensor reported by Alshehria et al.[31] Yet another way to obtain the absolute sprung-mass velocity is to design an observer.

Conclusion

In this paper, an active suspension system that can estimate the uncertainties and the effect of the road profile is proposed. The proposed control is SMC based on IDC and overcomes the drawback of conventional SMC which requires the bounds of the uncertainty and the disturbances. The efficacy of the proposed scheme is verified by simulation for a variety of road profiles. The results show that the proposed scheme is significantly better than the passive suspension system in improving the ride comfort. The accuracy of estimation is improved further with second-order IDC. The control is simpler than other skyhook suspensions from the implementation point of view and works satisfactorily for a variety of road profiles without any change in control.

Funding

This research received no specific grant from any funding agency in the public, commercial or not-for-profit sectors.

References

1. Hrovat D. Applications of optimal control to advance automotive suspension design. *Automatica* 1993; 115: 328–342.
2. Fialho I and Balas GJ. Road adaptive active suspension design using linear parameter-varying gain-scheduling. *IEEE Trans Control Systems Technol* 2002; 10: 43–54.
3. Alleyen A and Hedrick JK. Nonlinear adaptive control of active suspensions. *IEEE Trans Control Systems Technol* 1995; 3: 845–860.
4. Truscott AJ. Composite active suspension for automotive vehicles. *Comput Control Engng J* 1994; 5: 149–154.
5. Rajamani R and Hedrick J. Adaptive observers for active automotive suspensions: theory and experiment. *IEEE Trans Control Systems Technol* 1995; 3: 86–93.

6. Al-Holou N, Lahdhiri T, Joo DS et al. Sliding mode neural network inference fuzzy logic control for active suspension systems. *IEEE Trans Fuzzy Systems* 2002; 10: 234–246.
7. Esat II, Saud M and Engin SN. A novel method to obtain a real-time control force strategy using genetic algorithms for dynamic systems subjected to external arbitrary excitations. *J Sound Vibr* 2011; 330: 27–48.
8. Lin J, Lian R-J, Haung C-N and Sie W-T. Enhanced fuzzy sliding mode controller for active suspension systems. *Mechatronics* 2009; 19; 1178–1190.
9. Sunwoo M, Cheok KC and Huang N. Model reference adaptive control for vehicle active suspension systems. *IEEE Trans Ind. Electron* 1991: 38; 217–222.
10. Mohan B and Phadke SB. Variable structure active suspension system. In: *IEEE 22nd international conference on industrial electronics, control, and instrumentation*, Taipei, Republic of China, 5–10 August 1996, vol. 3, pp. 1945–1948. New York: IEEE.
11. Mohan B, Modak JP and Phadke SB. Vibration control of vehicles using model reference adaptive variablestructure control. *Adv Vibr Engng* 2003; 2: 343–361.
12. Kim C and Ro PI. A sliding mode controller for vehicle active suspension systems with non-linearities. *Proc IMechE Part D: J Automobile Engineering* 1998; 212: 79–92.
13. Utkin V. *Sliding modes in control and optimization*. New York: Springer, 1992.
14. DeCarlo R, Zak S and Matthews G. Variable structure control of nonlinear multivariable systems: a tutorial. *Proc IEEE* 1988; 76: 212 –232.
15. Chen PC and Huang AC. Adaptive sliding mode control of non-autonomous active suspension systems with time-varying loading. *J Sound Vibr* 2005; 282: 1119–1135.
16. Chen H-Y and Huang S-J. Functional approximation-based adaptive sliding control with fuzzy compensation for an active suspension system. *Proc IMechE Part D: J Automobile Engineering* 2005; 219: 1271–1280.
17. Yoshimura T, Kume A, Kurimoto M and Hing J. Construction of an active suspension system of a quarter car model using the concept of sliding mode control. *J Sound Vibr* 2001; 239: 187–199.
18. Youcef-Toumi K and Ito O. A time delay controller for systems with unknown dynamics. *Trans ASME, J Dynamic Systems Measmt Control* 1990; 112: 133–142.
19. Zhong Q-C and Rees D. Control of uncertain LTI systems based on an uncertainty and disturbance estimator. *Trans ASME, J Dynamic Systems Measmt Control* 2004; 126: 905–910.
20. Talole SE and Phadke SB. Model following sliding mode control based on uncertainty and disturbance estimator. *Trans ASME, J Dynamic Systems Measmt Control* 2008: 130: 034 501.
21. Deshpande VS and Phadke SB. Control of uncertain nonlinear systems using an uncertainty and disturbance estimator. *Trans ASME, J Dynamic Systems Measmt Control* 2012; 134: 024 501.
22. Chen W. Nonlinear disturbance observer-enhanced dynamic inversion control of missiles. *J Guidance, Control Dynamics* 2003; 26: 161–166.
23. Deshpande VS and Phadke SB. Sliding mode control of active suspension systems using an uncertainty and disturbance estimator. In: *1st international conference on computational intelligence and information technology*, Communications in Computer and Information Science, Vol 250 (V Das and N Thankachan eds), Pune, India, 7–8 November 2011, pp. 15–20. Berlin: Springer, 2011.
24. Ackermann J and Utkin VI. Sliding mode control design based on Ackermann's formula. *IEEE Trans Autom Control* 1998; 43: 234–237.
25. Trench WF. *Introduction to real analysis*. Upper Saddle River, NJ: Pearson Education, 2003.
26. Chen PC and Huang AC. Adaptive sliding control of active suspension systems with uncertain hydraulic actuator dynamics. *Veh System Dynamics* 2006; 44: 357–368.
27. Chen BC, Shiu YH and Hsieh FC. Sliding-mode control for semi-active suspension with actuator dynamics. *Veh System Dynamics* 2001; 49(1–2): 277–290.
28. Williams RA. Automotive active suspensions. Part 1: basic principles. *Proc IMechE Part D: J Automobile Engineering* 1997; 211: 415–426.
29. Lin J, Lian RJ, Huang CN and Sie WT. Enhanced fuzzy sliding mode controller for active suspension systems. *Mechtronics* 2009; 19: 1178–1190.
30. Preumont A, Francois A, Bossens F and Abu-Hanieh A. Force feedback versus acceleration feedback in active vibration isolation. *J Sound Vibr* 2002; 257: 605–613.
31. Alshehri A, Gardonio P, Elliott S et al. Experimental evaluation of a two degree of freedom capacitive MEMS sensor for velocity measurements. *Procedia Engng* 2011; 25: 619–622.

Appendix

Notation

c_i	constants of the non-linear damper
c_s	linear damper coefficient of the skyhook reference model
c_{sky}	skyhook linear damper coefficient
e	lumped uncertainty
$\hat{e}$	estimate of the lumped uncertainty
$\tilde{e}$	estimation error
f_d	non-linear damping force
f_{d0}	nominal non-linear damping force
f_s	non-linear spring force
f_{s0}	nominal non-linear spring force
f_t	tyre force
$G_f(s)$	inertial delay filter
k_i	constants of the non-linear spring
k_s	linear spring coefficient of the skyhook reference model
K	positive constant
m_s	nominal sprung mass
m_{sm}	sprung mass of the skyhook reference model
m_u	nominal unsprung mass
m_{um}	unsprung mass of the skyhook reference model
M	constant matrix
N	constant matrix
P	positive definite matrix
r	positive constant
u	control force generated by the actuator
x_i	states of the suspension system

x_r	road profile relative to plane ground
x_s	displacement of the sprung mass relative to its static position
x_{sm}	displacement of the sprung mass of the skyhook reference model relative to its static position
x_u	displacement of the unsprung mass relative to its static position
x_{um}	displacement of the unsprung mass of the skyhook reference model relative to its static position
z	auxiliary variable in the definition of the sliding surface
Δx	suspension deflection
λ	positive constant
λ_1	positive constant
μ	positive constant
σ	sliding surface
τ	time constant of the inertial delay filter